

MODELING RHEOLOGY IN THE HOT-PRESSING OF MDF: COMPARISON OF MECHANICAL MODELS

Luisa M. H. Carvalho

Coordinator Professor
Department of Wood Engineering, Polytechnic Institute of Viseu
3500 Viseu, Portugal

Mário Rui N. Costa

Associate Professor
Laboratory of Separation and Reaction Engineering

and

Carlos A. V. Costa

Professor
Laboratory of Process, Environment and Energy Engineering
University of Porto
4200-465 Porto, Portugal

(Received June 2000)

ABSTRACT

The hot-pressing operation is the final stage in the MDF manufacture where the mattress of fibers is compressed and heated to promote the cure of the resin. The press cycle has a major effect on the balance of properties of the resulting panel, so rigorous control of all processing variables is necessary to improve product quality and to reduce pressing time. The rheological behavior of the mattress during pressing involves complex phenomena that are dependent on temperature, moisture content, gas pressure, and density distributions. Following a three-dimensional model of heat and mass transfer already built, mechanical models were developed to describe the viscoelastic behavior of the material. The elastic and viscous properties for the wood-resin composite were estimated based upon several kinds of "rules of mixtures," taking into account the relationship with the simulations already undertaken for temperature, moisture content, and gas pressure profiles, as well as the adhesive polymerization. These dynamic models were used to predict the evolution of compression stress, strain, modulus of elasticity, and density with time at a given position in the mattress, as well as the density profiles. The models were compared in relation to the influential factors affecting the composite compressibility. The simulation results are useful to identify the controlling factors of a hot-pressing operation and to understand better the complex mechanisms involved in panel formation.

Keywords: MDF, modeling, viscoelastic behavior, cellular materials, wood-based panels, hot-pressing.

INTRODUCTION

An important issue concerning MDF pressing is the integrated understanding of various phenomena: the heat and mass transfer, the polymerization of the adhesive, and the rheological behavior. This will permit the development of procedures that at design and operating levels allow for energy savings and avoid raw material losses by improved quality and increased operational flexibility. The press cy-

cle scheduling to fulfill the above objectives demands the development of predictive models that will enable the optimization and control of this operation. Unfortunately, the work in this field is very scarce, even for other wood-based panels, and does not integrate all the mechanisms involved (Humphrey and Bolton 1989; Hata et al. 1990).

The rheological behavior of the mattress during pressing is quite complex: the stresses

developed due to densification can be relaxed, blocked in the solid structure, released, or originate elastic deformation. These physical processes are tightly coupled with temperature and humidity distributions; the density profile affects the heat and steam fluxes across the mattress porous structure (Wolcott et al. 1990; Bolton et al. 1989). On the other hand, as the resin cures, it is expected that an increase of stress relaxation takes place, because of the formation of a network structure that promotes the development of a uniform distribution of stresses.

To understand the consolidation process, it is necessary to know the behavior of the individual elements in transverse compression. Unfortunately, even for lumber, there are almost no rheological data that can be used at the operating conditions of particleboard or fiberboard production. Nevertheless, it is known that under these conditions these materials have a viscoelastic behavior.

Several publications have dealt with a theoretical description of the mechanical behavior during the pressing of wood-based panels (Harless et al. 1987; Dai and Steiner 1993; Suo and Bowyer 1994; Lang and Wolcott 1996; Lenth and Kamke 1996b). However, to simplify the understanding of this complex mechanism, they separate the nonlinear response of the material to compression from its viscoelastic behavior. Only the first subject is treated and the models deal only with the stress-strain behavior of the mattress of wood particles during consolidation, neglecting the influence of resin polymerization. Besides, very little work has been done to characterize the network of this type of cellular structures (Lenth and Kamke 1996a).

The heat and mass transfer is included in only two models, where only conduction and diffusion are considered. Harless et al. (1987) developed a model to predict the vertical density profile of particleboard by simulating the hot-pressing process. However, the compressibility was modeled from experimental data obtained in a laboratory-scale press, with mats of particles without resin. Suo and Bowyer

(1994) also have made an attempt to model the vertical density profile together with temperature and moisture content during the hot-pressing of particleboard. This model was based on the compressibility and the resulting strain of each layer of the board thickness due to pressing, assuming elastic behavior.

The compressive stress-strain behavior has been modeled by some authors using a statistical approach (Dai and Steiner 1993; Lang and Wolcott 1996) or a mechanistic approach (Lenth and Kamke 1996b). The model of Dai and Steiner (1993) was developed for a randomly formed flake mat, and the linear and nonlinear stress-strain relationships for wood were modeled by Hooke's law, modified with a nonlinear strain function that was experimentally determined. Lang and Wolcott (1996) presented a theoretical model for a randomly formed wood-strand mat, and the stress development was also governed by the modified Hooke's law.

Lenth and Kamke (1996b) tested the applicability of design theories to predict compressive stress-strain behavior of cellular materials for modeling the consolidation of a wood flake mat. The mechanical response to compression of cellular materials as honeycomb, open and closed foams, cork, and wood is nonlinear, resulting from the collapse of the cellular structure. The typical deformation process goes through three phases: initial cell-wall bending (linear elastic regime), nonlinear collapse of the cellular structure (yielding plateau), and finally densification of the cell wall (sharp increase in stress), after the majority of cell walls have collapsed. These theories, originally developed by Gibson and Ashby (1988) for cellular materials, were applied by Wolcott et al. (1989) to model the stress-strain behavior of wood particles in transverse compression under different temperature or moisture content conditions and can be applied, as Lenth and Kamke (1996b) have demonstrated, to the consolidation of wood particles mats.

The viscoelastic response during the hot-pressing is not considered in these models. Wood and wood-based composites exhibit

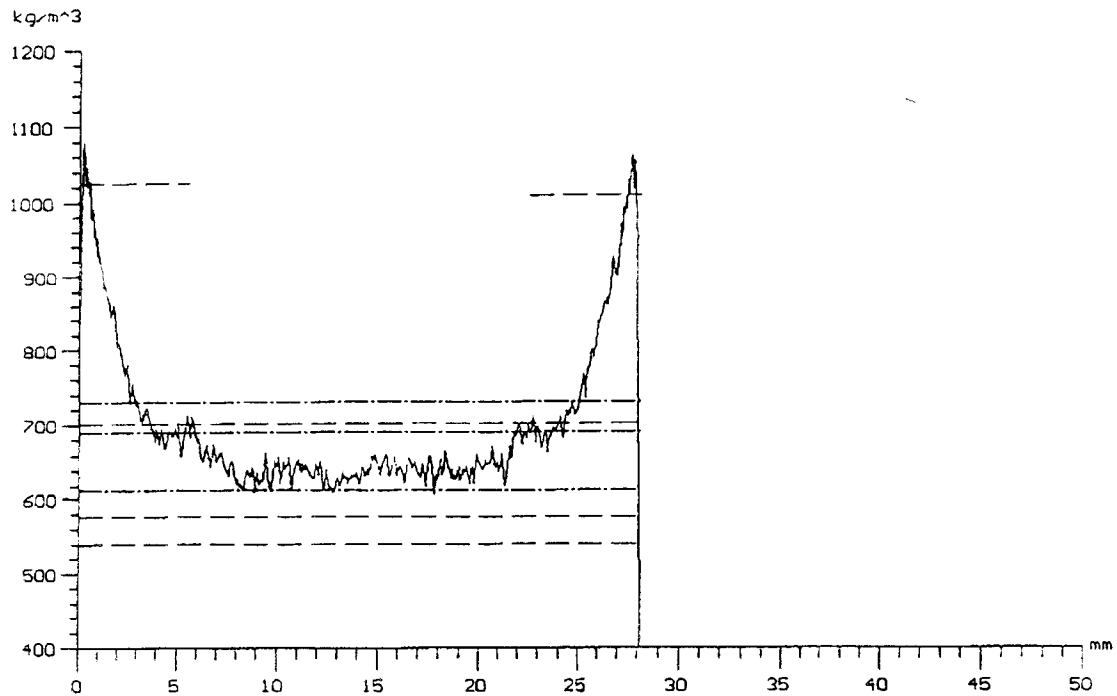


FIG. 1. Density profile for an MDF sample.

within certain levels of stress, linear elastic behavior (Bodig and Jayne 1982). So, the viscoelastic behavior of these materials can be represented by a combination of linear responses, elastic (Hookean) and viscous (Newtonian), and the total strain can be considered as the sum of independent elastic (springs) and viscous (dashpots) components (Ward and Hadley 1993). The rheological behavior of wood and its composites has been studied by creep and relaxation experiments. The Burger model was used to describe the creep behavior of particleboard (Dinwoodie et al. 1984) and also of urea formaldehyde resin (Irlle and Bolton 1991) at ambient conditions. Among the models generally used to describe the stress relaxation, the most important are the Maxwell model and the standard linear solid. Unfortunately, there is very little published information at high temperatures and over the range of moisture contents experienced in particleboard or fiberboard manufacture to estimate the spring and dashpot constants.

The rheological behavior of wood composites can be viewed at two levels: the macromechanics and the micromechanics scales. At macromechanics scale, the models are constructed based on the type of geometry and orientation of the elements in the board. The aim of micromechanics is to predict the mechanical properties of each element from the mechanical properties of its constituents. From this standpoint, we present and discuss two macromechanical models for the hot-pressing of MDF, and the parameters of these models are predicted using the approach of micromechanics.

THE STRUCTURE OF MDF

Figure 1 shows a density profile for an MDF sample, obtained using gamma-ray attenuation. The shape of this curve reveals high-density face layers and low-density core layers. This is a typical vertical density profile for MDF boards manufactured by the conven-

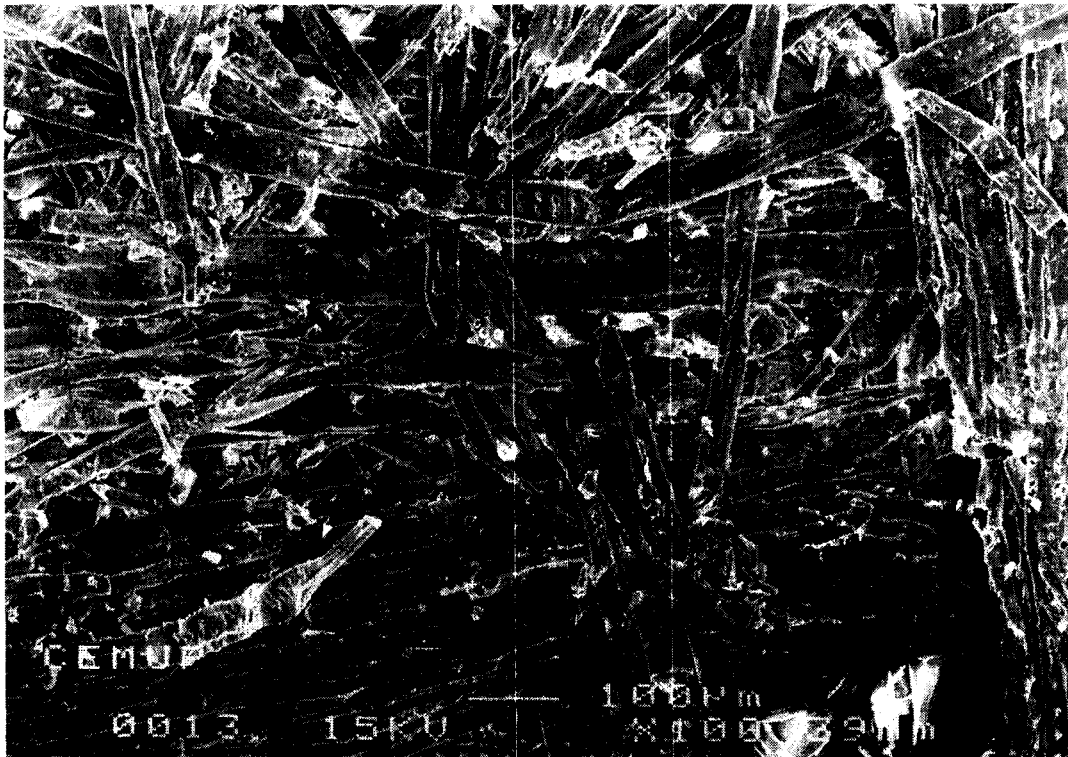


FIG. 2. Failure surface exposed of an MDF sample subjected to an internal bond test, obtained using SEM (magnification is $\times 100$).

tional pressing process. However, the panel may take on other profiles depending on pressing conditions.

The MDF panel used in this investigation was manufactured with *Pinus pinaster* fibers bonded with urea-formaldehyde resin (resin content = 8.5% mass of resin/mass of oven-dry fiber; final board density = 750 kg/m³). In Fig. 2 we can observe the delaminated surface of an MDF sample subjected to an internal bond test (EN 319). The objective was not the characterization of the fracture zone, in terms of fiber or resin bridges failure, as in Butterfield et al. (1992), but mostly regarding the distribution and orientation of the fibers. The SEM observations indicated that most of the fibers and fiber bundles are randomly oriented within horizontal planes, parallel to the surface. This structure is a direct consequence of the forming and pressing operations, but also of the fiber morphology, deformation, slip-

ping, intersection, and the settlement of resin bridges.

The MDF is a porous structure, thus meaning that board porosity is an important parameter in the development of a rheological model. A Pore Sizer Micromeritics 9320 was used, and the porosity obtained was 48.3% for an MDF sample with 10 \times 10 \times 12 mm.

MODEL DEVELOPMENT AND NUMERICAL SOLUTION

As a first approach, a mechanical model was developed assuming elastic behavior (Carvalho 1999). Although this model does not represent the whole press cycle, it is important to understand the press closing period, when the stress relaxation can be neglected. After the press closure, the stress relaxation is important, and the mattress presents a visco-elastic behavior. To describe this behavior, we

considered a Maxwell model (Drozdov 1998). The model does not include directly heat and mass transfer; but the conditions of temperature, moisture content, relative humidity, and gas pressure were estimated from the results of a three-dimensional heat and mass transfer model (Carvalho and Costa 1998), using cubic splines interpolation. The model also includes the influence of the resin cure in the elastic properties. At the beginning and during the press cycle, a position control is usually used in the industry; the load is applied following a program of the mat thickness or the platen position. So the model performance will be analyzed, imposing a perturbation in the thickness (or total strain) and observing the response in stress.

In model construction, we considered the following assumptions:

1. The consolidation of the fiber mattress occurs in the vertical direction and no lateral expansion is considered;
2. For the elastic model, elastic behavior during the whole press-cycle; for the viscoelastic model, linear viscoelastic during the whole press-cycle;
3. The mechanical properties of the board (moduli of elasticity and viscous components) are functions of local temperature, moisture content, density, and the development of stiffness due to adhesive cure.
4. Position control during the press cycle: a perturbation in thickness (or total strain) is imposed and the response in stress is observed.

The elastic model contains four dependent variables (vertical position z , overall compressive stress σ_T , overall modulus of elasticity $\langle E \rangle$, and local strain $\epsilon_{i,j,k}$) and four governing equations: one for the calculation of the overall elasticity modulus from every local modulus of elasticity (Eq. 8); one equation that relates the vertical position and local strain (Eq. 10), and Hooke's law to calculate the overall stress (Eq. 6) and the local strain (Eq. 11). The viscoelastic model contains an additional variable, the overall viscous component

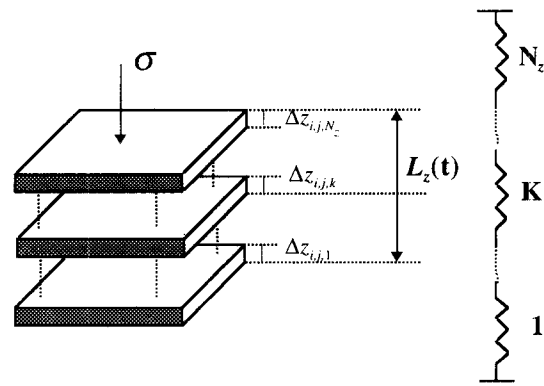


FIG. 3. A column of the board consisting of N_z layers.

$\langle \mu \rangle$ and an additional equation to calculate the overall viscous component from every local viscous component (Eq. 9). Hooke's law is substituted by the Maxwell model to calculate the overall stress (Eq. 7) and the local strain (Eq. 12). Globally, the board is modeled considering a generalized Maxwell model (several Maxwell elements in series).

Although the two surfaces in contact with the press platens can experience slightly different conditions, we assume geometric symmetry in order to save computing time. There are three planes of symmetry; thus only the events in one eighth of the board need to be modeled. This one eighth is divided in $N_x \times N_y$ columns, each one with N_z layers (see Fig. 3) making a total of $N_x \times N_y \times N_z$ control volumes. In "z" direction, K is the spatial index of each control volume that varies from 1 to N_z , (number of control volumes). Δz is the thickness of each control volume, and L_z is the board half thickness that varies with time. Assuming that a uniform compressive stress is applied to the board in the z direction, the stress will be the same for each layer, and the total thickness of each column will be equal to the sum of individual thickness of all layers. So, the elasticity modulus of each column can be calculated using the rule of mixtures. Considering that all the columns will be subjected to equal stress, the overall elasticity modulus can be calculated as the average of the elasticity modulus of all columns ij .

When the mattress of fibers is subjected to mechanical pressure, the board thickness will change with time, as well as the vertical position (z). In order to fix the domain of integration, we adopted a transformation, introduced by Landau and Lewis (1950), which will be useful for the construction of a global model that integrates the heat and mass transfer and the mechanical behavior:

$$Z = \frac{z}{L_z(t)} \tag{1}$$

We considered the following variables and parameters that will appear in the constitutive model equations:

$$\begin{aligned} L_z^* &= \frac{L_z}{L_{z_0}} & \theta &= \frac{t}{\tau} \\ \Delta Z_{i,j,k} &= \frac{\Delta z_{i,j,k}}{L_z^* L_{z_0}} & \Delta Z_0 &= \frac{\Delta z_0}{L_{z_0}} = \frac{1}{N_z} \\ \sigma_T^* &= \frac{\sigma_T}{\sigma_{T_0}} & E_{i,j,k}^* &= \frac{E_{i,j,k}}{E_0} & \mu^* &= \frac{\mu}{\mu_0} \end{aligned}$$

where L_{z_0} is the initial board half thickness, τ the press cycle time, and Δz_0 the reference (initial) thickness, σ_{T_0} is the reference compressive stress, E_0 is the reference modulus of elasticity, and μ_0 the reference viscous component. From now on $L_z(t)$ will be represented just by L_z . We also considered the following dimensionless numbers:

$$Ho = \frac{E_0}{\sigma_0} \quad Vi = \frac{E_0 \tau}{\mu_0}$$

The overall and local strains can be calculated by:

$$\epsilon = \frac{L_z}{L_{z_0}} - 1 = L_z^* - 1 \tag{2}$$

$$\epsilon_{i,j,k} = \frac{\Delta z_{i,j,k}}{\Delta z_0} - 1 = \frac{\Delta Z_{i,j,k} L_z^*}{\Delta Z_0} - 1 \tag{3}$$

The strain distribution will depend on the compressibility of each element (control volume). In order to calculate the position of each element, it is necessary to know the strain of

this element and of those situated below, in the same column. In agreement with Fig. 3, the strain of each layer will depend on the strain of the underneath layers:

$$\epsilon_{i,j,k} = 2 \frac{z_{i,j,k}}{\Delta z_0} - 1 - 2 \left[\sum_{l=1}^{k-1} (\epsilon_{i,j,l} + 1) \right] \tag{4}$$

and the vertical position z , corresponding to the centroid of each control volume, can be related with the strain, through the following expression:

$$z_{i,j,k} = \frac{\Delta z_0}{2} \left(\epsilon_{i,j,k} + 2 \sum_{l=1}^{k-1} \epsilon_{i,j,l} + 2K - 1 \right) \tag{5}$$

The constitutive equations for the elastic and viscoelastic models, in dimensionless form, are the following:

Elastic model:

$$\frac{\partial \sigma_T^*}{\partial \theta} = Ho \langle E^* \rangle \frac{\partial L_z^*}{\partial \theta} \tag{6}$$

Viscoelastic model:

$$\frac{\partial \sigma_T^*}{\partial \theta} = Ho \langle E^* \rangle \frac{\partial L_z^*}{\partial \theta} - Vi \frac{\langle E^* \rangle}{\langle \mu^* \rangle} \sigma_T^* \tag{7}$$

$$\langle E^* \rangle = \frac{1}{N_x N_y} \sum_{ij} E_{ij}^*$$

$$E_{ij}^* = \frac{1}{\Delta Z_0} \frac{1}{\sum_{k=1}^{N_z} \frac{1}{E_{i,j,k}^*}}$$

$$\langle \mu^* \rangle = \frac{1}{N_x N_y} \sum_{ij} \mu_{ij}^*$$

$$\mu_{ij}^* = \frac{1}{\Delta Z_0} \frac{1}{\sum_{k=1}^{N_z} \frac{1}{\mu_{i,j,k}^*}} \tag{8}$$

IC: $\sigma_T^* = 0 \quad L_z^*(\theta) = 1 \tag{9}$

The time derivative of Eq. 5 yields:

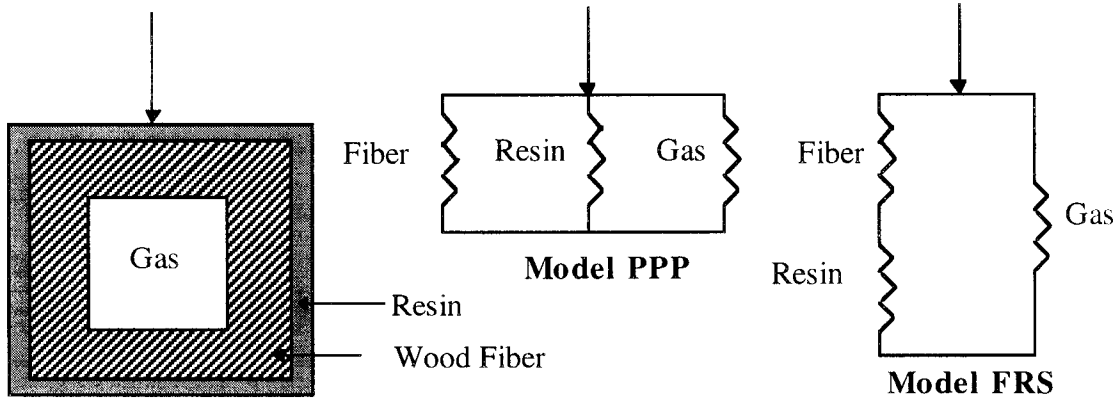


FIG. 4. Cell model and micromechanical models for MDF.

$$\frac{\partial Z_{i,j,k}}{\partial \theta} = \frac{\Delta Z_0}{2L_z^*} \left(\frac{\partial \epsilon_{i,j,k}}{\partial \theta} + 2 \sum_{l=1}^{k-1} \frac{\partial \epsilon_{i,j,l}}{\partial \theta} \right) - \frac{Z_{i,j,k}}{L_z^*} \frac{\partial L_z^*}{\partial \theta} \quad (10)$$

$$\Delta Z_{i,j,k} = 2 \left(Z_{i,j,k} - \sum_{l=1}^{k-1} \Delta Z_{i,j,l} \right) \quad (15)$$

Mechanical properties: micromechanical models

Elastic model:

$$\frac{\partial \epsilon_{i,j,k}}{\partial \theta} = \frac{1}{HoE_{i,j,k}^*} \frac{\partial \sigma_T^*}{\partial \theta} \quad (11)$$

Visoelastic model:

$$\frac{\partial \epsilon_{i,j,k}}{\partial \theta} = \frac{1}{HoE_{i,j,k}^*} \frac{\partial \sigma_T^*}{\partial \theta} + \frac{Vi}{E_0} \frac{\sigma_T^*}{\mu_{i,j,k}^*}$$

IC: $Z_{i,j,k} = \frac{K - 0.5}{N_z} \quad \epsilon_{i,j,k} = 0 \quad (12)$

The density of each control volume can be obtained by a mass balance. As there is no interlayer transport of solid material, the mass of the solid material in each volume element remains unchanged during compression, that is:

$$\rho_c = \rho_{c_0} \frac{\Delta z_0}{\Delta z} \quad (13)$$

where ρ_{c_0} is the reference density. The equation in dimensionless form is:

$$\rho_{ci,j,k}^* = \frac{\Delta Z_0}{\Delta Z_{i,j,k} L_z^*} \quad (14)$$

with:

At the micromechanics scale, the Young’s modulus for the wood-resin composite can be estimated based upon the “rule of mixtures,” usually used in the theoretical analysis of composite materials (Agarwal and Broutman 1990), taking into account the contributions of each constituent: the wood fiber, the resin, and the gas (air and steam) present in the voids. To predict the composite elasticity modulus, we considered two micromechanical models, one with three components in parallel, and in the other model, the solid is composed of fiber and resin in series and the gas in parallel (see Fig. 4).

For the parallel model (PPP), a longitudinal “rule of mixtures” can be applied. So the elastic modulus of the solid (fiber + resin) can be written as follows:

$$E_s = V_f E_f + V_r E_r \quad (16)$$

where E_f and E_r are, respectively, the Young’s moduli of the fiber and resin; V_f and V_r are the fiber and resin volume fractions.

Considering the elements in series (model FRS), the solid elastic modulus may be obtained using a transverse “rule of mixtures”:

$$\frac{1}{E_s} = \frac{V_f}{E_f} + \frac{V_r}{E_r} \quad (17)$$

or the Halpin-Tsai (Halpin and Tsai 1969) equation, that is a modification of the rule of mixtures formulation to account for fiber discontinuities and packing orientation:

$$E_s = E_r \frac{1 + \xi \eta V_f}{1 - \eta V_f} \quad (18)$$

where

$$\eta = \frac{E_f/E_r - 1}{E_f/E_r + \xi}$$

with ξ equal to 2.

The transversal and longitudinal "rule of mixtures," as well as the Halpin-Tsai equation, have already been applied to predict the modulus of elasticity of other wood-based panels (Shaler and Blankenhorn 1990).

To calculate the elasticity modulus of the gas mixture (steam + air) entrapped in the voids, it should be noted that the system is not closed: there is a gas flow through the porous media. In a previous publication (Carvalho and Costa 1998), an increase in gas pressure was noticed at the beginning of the press cycle, because the rate of steam production was larger than the rate of steam lost through board edges. Due to the decrease of thickness, the gas pressure will increase even more. Neglecting the lateral deformation of the mattress, the modulus for the gas can be calculated by:

$$E_g = \frac{P - P_0}{\epsilon} \quad (19)$$

where P is the total gas pressure and P_0 the initial pressure.

The composite modulus can then be calculated by:

$$E_c = V_s E_s + V_g E_g \quad (20)$$

and the volume fractions by:

$$V_s = \frac{\rho_c}{\rho_s} \quad V_g = 1 - V_s \quad (21)$$

where ρ_c is the apparent density of the composite and ρ_s the real density of the solid.

The influence of relative density (apparent density to solid material density) in the light of the cellular solids theory was also considered (Gibson and Ashby 1988). For the elastic compression of a honeycomb, the Young's modulus can be expressed as a function of the cell-wall modulus of the material (E_s), a linear elastic constant (C_2), and the relative density:

$$E_c = C_2 E_s \left(\frac{\rho_c}{\rho_s} \right)^3 \quad (22)$$

The response of wood when loaded across the grain is analogous to a honeycomb, and the same relationship was observed by Gibson and Ashby (1988). The linear elastic constant (C_2) includes all the geometric constants of proportionality. Wolcott et al. (1989) have demonstrated that C_2 decreases with sample thickness, taking values from 1, for samples with thickness larger than 40 mm to 0.015 for particles with 0.9 mm. Lenth and Kamke (1996b) obtained 0.05 for the compression of particle mats.

Considering the same modeling approach, Eq. (20) may be written as follows:

$$E_c = C_2 E_s \left(\frac{\rho_c}{\rho_s} \right)^3 + E_g \left(1 - \frac{\rho_c}{\rho_s} \right) \quad (23)$$

The combination of models PPP or FRS with the relationship derived for a honeycomb is obtained calculating E_s in Eq. (23) with Eqs. (16) and (17) (or 18), respectively.

To predict the whole stress-strain curve, Wolcott et al. (1989) proposed a modified Hooke's law with a non-linear strain function $\Phi(\epsilon)$, and Eq. (23) is rewritten as:

$$E_c = C_2 E_s \left(\frac{\rho_c}{\rho_s} \right)^3 \Phi(\epsilon) + E_g \left(1 - \frac{\rho_c}{\rho_s} \right) \quad (24)$$

with

$$\Phi(\epsilon) = \frac{C_3/C_2}{\epsilon} \left[\frac{1 - \left(\frac{\rho_c}{\rho_s} \right)^{1/3}}{1 - \left(\frac{\rho_c}{\rho_s} \frac{1}{1 - \epsilon + \epsilon_y} \right)^{1/3}} \right]^3 \quad (25)$$

where C_3 is equal to the yield strain (ϵ_y). When ϵ is less or equal to the yield strain (ϵ_y), $\Phi(\epsilon)$ is equal to unity (initial linear compression range). For the compression of wood particles or columns of wood particles, the yield stress is around 0.14–0.16 (Wolcott et al. 1989; Dai and Steiner 1993).

The Young's modulus of wood fiber was calculated using data from Wolcott et al. (1990) obtained for wood cell-wall considering several conditions of temperature and moisture content and fitted with the following equation:

$$E_f = E_{f_0} \exp\left(-\frac{\beta_T}{T + T_0} + \frac{\beta_H}{H - H_0}\right) \quad (26)$$

with parameters: $\beta_T = -1,820^\circ\text{C}$, $\beta_H = 0.0695$, $T_0 = 447^\circ\text{C}$, $H_0 = 0.2925$, $E_{f_0} = 674$ MPa.

In the absence of experimental data for the evolution of the Young's modulus during the hardening of resin, it was decided to use data from Yin (1994) obtained in a TMA using two strips of wood bonded with urea-formaldehyde and loaded in bending. In order to withdraw the variability of wood, Yin (1994) considered a relative modulus of elasticity for the wood-resin composite:

$$E_{rel} = \frac{E - E_{min}}{E_{max} - E_{min}} \quad (27)$$

that changes from a minimum (1,000 MPa), at ambient temperature to a maximum (5,000 MPa), at 200°C . The continuous function that leads to the best fit is:

$$E_{rel} = \tanh(\exp(AT + B)t^n) \quad (28)$$

with parameters: $A = 0.246789 \text{ s}^{-1} \text{ K}^{-1}$, $B = -92.562 \text{ s}^{-1}$, $n = 3.859114$. T is the temperature in K and t is time in min. The resin modulus can be expressed as:

$$E_r = E_{rel} \times 1,000 \quad (29)$$

The viscous component for wood-resin required for the viscoelastic model was estimated using an additive mixing rule, that is being used for copolymers and polymer blends (Chartoff 1997):

$$\mu_s = W_f \mu_f + W_r \mu_r \quad (30)$$

where W_f and W_r are the weight fractions of wood fiber and resin, respectively.

It is difficult to find useful experimental data for the viscous components of wood fiber and UF resin at the conditions observed during hot-pressing.

For wood fibers, a few attempts have been made to clarify the effect of temperature and moisture content on its viscoelastic behavior (Salmen 1982), but only Wolcott et al. (1990) were concerned with the conditions encountered in the hot-pressing of wood composites. They considered an indicator of this behavior: the difference between temperature inside a flake mat and the glass transition temperature (T_g) of hemicellulose and lignin predicted, using the Kwei equation derived for polymer blends (Chartoff 1997). Their analysis was restricted to the amorphous polymers in wood, because it is reasonable to consider that the semi-crystalline cellulose is not viscoelastic for the low levels of moisture content. In case of MDF, as a consequence of the defibrating process, the fiber and fiber bundles will have superficial layers rich in lignin, and excluding the presence of resin, the transition of lignin will dominate the behavior of this type of composite. Using the same approach, we tracked the $T_g - T$ of lignin through the press cycle of MDF for several positions in the matress. The conditions of temperature and moisture content were predicted from the results of the heat and mass transfer model (Carvalho and Costa 1998). We verified that the transition region (between -25 and 25°C) is not attained in any of these locations, which indicates that the majority of wood polymers should be in the glassy state (Carvalho 1999). Therefore, assuming that the time-temperature superposition principle (TTS) is valid, we can apply the Arrhenius equation that is usually used below T_g .

For UF resin, that is a thermosetting polymer, the time-temperature-transformation diagram is more complex, because two more transformations have to be considered: the ge-

lation and the vitrification. The viscosity will depend on temperature and polymerization reaction, but no correlation between this rheological property and the molecular properties predicted by a kinetic model was found in the literature for this adhesive. However, from a practical point of view, it is commonly used for thermosetting composites in transient state, and Arrhenius type equation that includes also a term to represent the influence of the resin cure (Hojjati and Hoa 1994):

$$\mu = \mu_{\infty} \exp \left[\frac{\Delta E_{\mu}}{RT} + d\alpha \right] \quad (31)$$

where μ_{∞} and d are constants, ΔE_{μ} is the activation energy for viscous flow and α is the degree of cure. In this equation, we notice two components: the viscous flow, represented by the Arrhenius equation and the resin hardening. The parameters of this equation can be determined experimentally, but it is not advisable to make predictions beyond the experimental conditions. The degree of cure of UF resin was determined using experimental data from Yin (1994).

Numerical method

This approach results in a nonlinear unsteady-state problem, and the resulting set of initial value differential equations was handled using the special stiff equations solver LSODES (Hindmarsh 1983). This solver uses the Gear method and treats the Jacobian matrix in general sparse form to avoid the computation of zero-valued Jacobian entries. For modeling purposed, we used the same grid as outlined by Carvalho and Costa (1998): one eighth of the board was discretized in 1,000 points, 10 in each direction, each grid point corresponding to a control domain. The parameters of LSODES were set according to the instructions; the Jacobian matrix was computed internally, and we set the relative error to $0,125 \times 10^{-4}$ and absolute error to $0,125 \times 10^{-6}$. The output data from the three-dimensional heat and mass transfer model were fitted using cubic splines interpolation (De Boor 1978).

RESULTS AND DISCUSSION

These dynamic models were used to predict the evolution of pressing pressure, strain, modulus of elasticity, and density with time at a given position in the mattress, as well as the density profiles. Several simulations were carried out to show the ability of the model to perform well in a fairly large range of parameters values. The elastic model was used to show the applicability of micromechanical models to estimate local properties. The typical operating conditions considered are: platen temperature = 190°C; press cycle time = 330 s; board final thickness = 19 mm; initial moisture content = 11%; resin content = 8.5%; initial board density = 230 kg/m³. The time is counted after the plate touches the board. In the case of the viscoelastic model, we made a sensitivity analysis of several parameters and properties, namely the viscous component, the Young's modulus of fiber, resin, and gas and also of the most important operating conditions: the platen temperature and the initial mattress moisture content.

The elastic model applies only at the beginning of the press cycle, and it was used to show the applicability of micromechanical models to estimate local properties (Carvalho 1999). Due to the structure of MDF, the classical approach of the "rule of mixtures" only gives accurate results considering the three elements (resin + wood fiber + gas) in parallel (model PPP). The application of the cellular solids theories in the prediction of the stress-strain curve was also tested. Figure 5 shows a comparison between micromechanical models PPP and FRS using the Eq. (23) to estimate the composite modulus.

We concluded that the model PPP, combined with the relationships derived for a honeycomb is fairly effective in predicting the influence of the density of porous structure during compression. The modified Hooke's law does not improve the quality of the results, having in mind the response of the real pressing system. So, it is more reasonable to con-

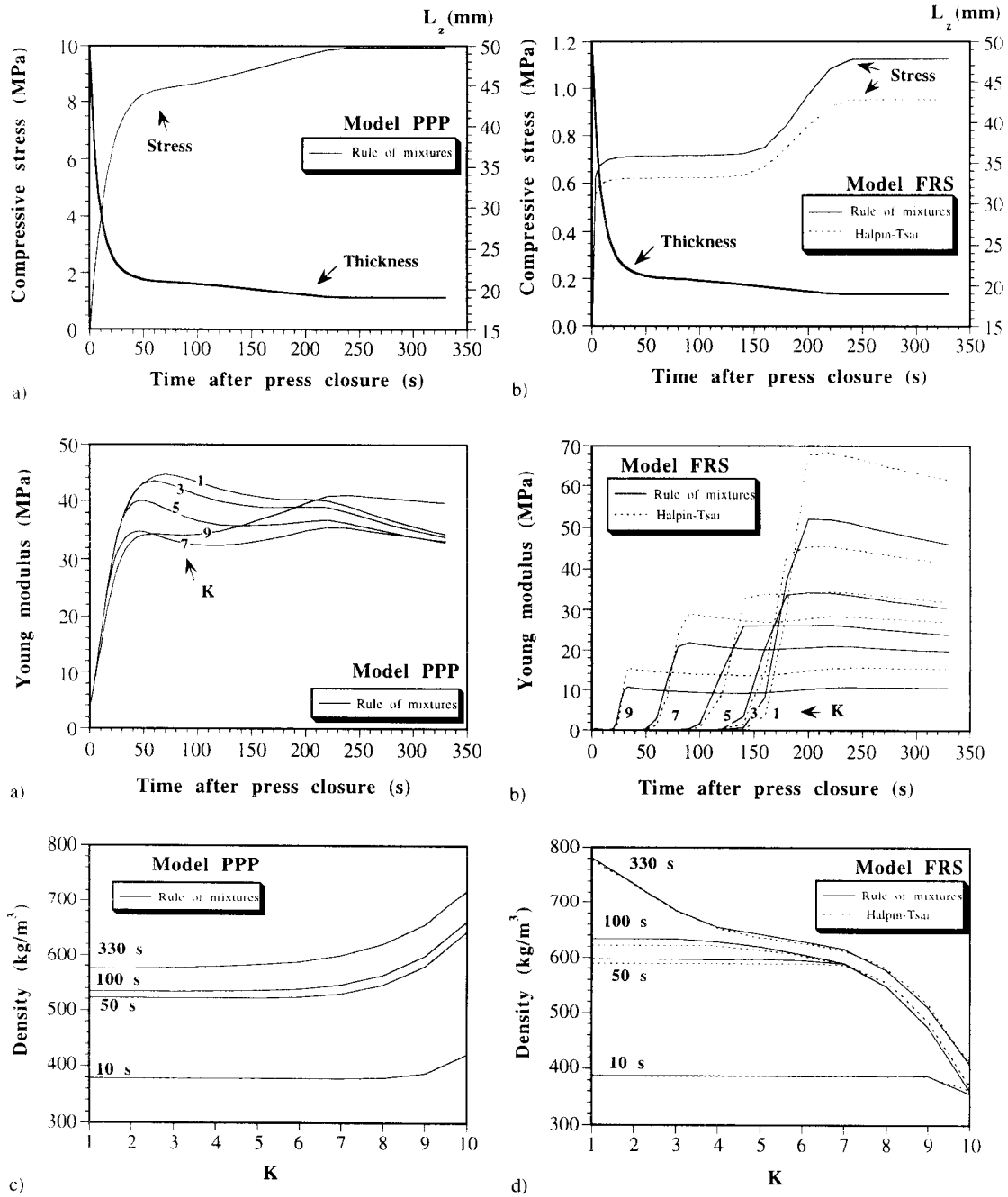


FIG. 5. Comparison between models PPP and FRS using the elastic model and the cellular solids theory for linear elastic behavior ($C_2 = 0.05$); a), b) evolution of overall compressive stress with time after press closure in response to a near step change in board thickness; c), d) evolution of the predicted Young's modulus at the central horizontal plane of the board with time after press closure for several positions in the vertical direction (numbered from $K = 1$ -adjacent to board mid-plane to $K = 10$ -adjacent to board surface); e), f) vertical profiles of density, along the z axis, at the board mid-plane for different times after press closure.

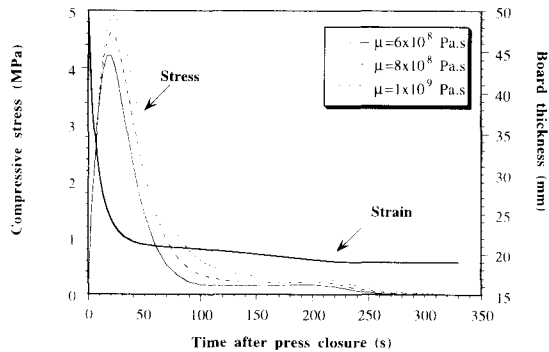


FIG. 6. Predicted (viscoelastic model) evolution of overall compressive stress with time after press closure in response to a near step change in board thickness, for different viscous components.

sider linear elastic behavior, because this equation is easier to handle (Carvalho 1999).

Unlike the elastic model, the viscoelastic model can be applied to the whole press cycle. In order to study the model performance, several simulations were performed changing the parameters and properties, starting with the viscous component. The micromechanical model used was the model PPP (the three elements in parallel) combined with the relationship derived for a honeycomb assuming linear elastic behavior, that proved to produce better results.

Figure 6 refers to the viscoelastic model and plots the response of the overall compressive stress to a perturbation in the board thickness, as a function of time at the central horizontal plane of the mattress and using the viscous component as a parameter.

The results indicate that the viscoelastic model allows a very accurate description of the evolution of overall compressive stress (or counterpressure) with time during press cycle, but this evolution is strongly dependent on the viscous component. For the values of viscous component presented, the results are very close in magnitude to those observed in an industrial pressing cycle. To gain some understanding on how operating parameters affect the model response, several simulations were carried out, changing the press temperature and the initial mattress moisture content. For

this purpose, the viscous component was settled to 8×10^8 Pa·s.

Figure 7 displays the results for three press temperatures: 190, 175, and 160°C. The effect of platen temperature on system responses in compressive stress is less important than expected, from the results of laboratory tests made with particle mattresses (Bolton et al. 1989). A possible explanation could be the fact that during the initial instants of press cycle, no difference is observed between the histories of the Young's modulus of the composite. On the other hand, these results do not take into account the influence of temperature on the viscous component. The effect on vertical density profile is more important, mostly at the end of press cycle and towards the surface. This plot agrees with the expected behavior: a higher press temperature implies a greater densification of the surface layers.

As foreseen above, the mattress moisture content has an important influence in all variables presented in Fig. 8. at levels usually used in the hot-pressing of wood-based panels. The lower the initial average mattress moisture content, the higher the pressure needed to attain the target thickness. An increase in board moisture content implies a larger compressibility and a larger possibility of fiber plasticization. The results for the density profiles along the board thickness confirm this behavior: an increase in mattress moisture content emphasizes the density differences between core and surface layers. It must be pointed out that the moisture content can also affect the resin polycondensation reaction, but this effect was not considered.

The model performance was analyzed for a variable viscous component. Figure 9 presents the influence of resin in the determination of the composite viscous component calculated by Eq. (30). For the fiber, an Arrhenius equation with the following parameters was used:

$$\mu_x = 1 \times 10^8 \text{ Pa}\cdot\text{s} \quad \Delta E_\mu = 3,241 \text{ J/mol}$$

The parameter μ_x was chosen after a sensitivity analysis and the activation energy (ΔE_μ) was obtained from experimental data

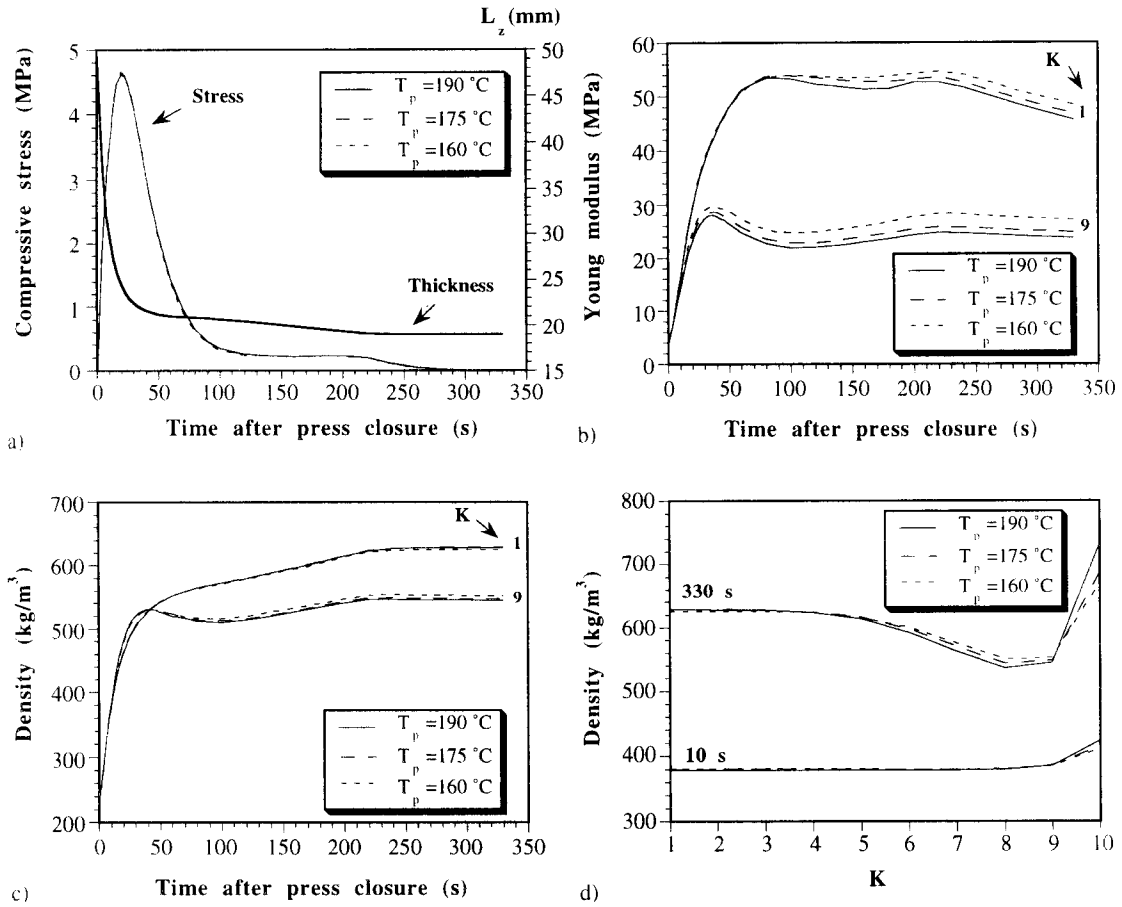


FIG. 7. Effect of platen temperature; evolution of a) overall compressive stress; b) Young's modulus; and c) density with time after press closure for several positions in the vertical direction (numbered from $K = 1$ -adjacent to board mid-plane to $K = 10$ -adjacent to board surface); d) vertical profiles of density, along the zz axis, at the board mid-plane for different times after press closure.

presented elsewhere (Yin 1984). The viscous component of the resin was calculated using Eq. (31). Acknowledging that these parameters are not available for the UF resin, we conducted a sensitivity analysis to feel the importance of these parameters on the system response, starting with the values for an epoxy resin (Hojjati and Hoa 1994):

$$\mu_{\infty} = 7.93 \times 10^{-14} \text{ Pa}\cdot\text{s}$$

$$\Delta E_{\mu} = 9.08 \times 10^4 \text{ J/mol} \quad d = 14.1$$

The inclusion of the resin contribution causes a decrease on the composite viscous component, although the curve of the evolution

with time has the same shape. As a consequence, the system response shows a slight decrease on the maximum compressive stress. The fact that we used an additive rule of mixtures and also the relative low resin content could explain these results. The replacement of this empirical approach with one more rigorous is highly desirable.

CONCLUSIONS

This paper presents a comparison between mechanical models for the simulation of the hot-pressing process in MDF cure.

A preliminary study of the structure of

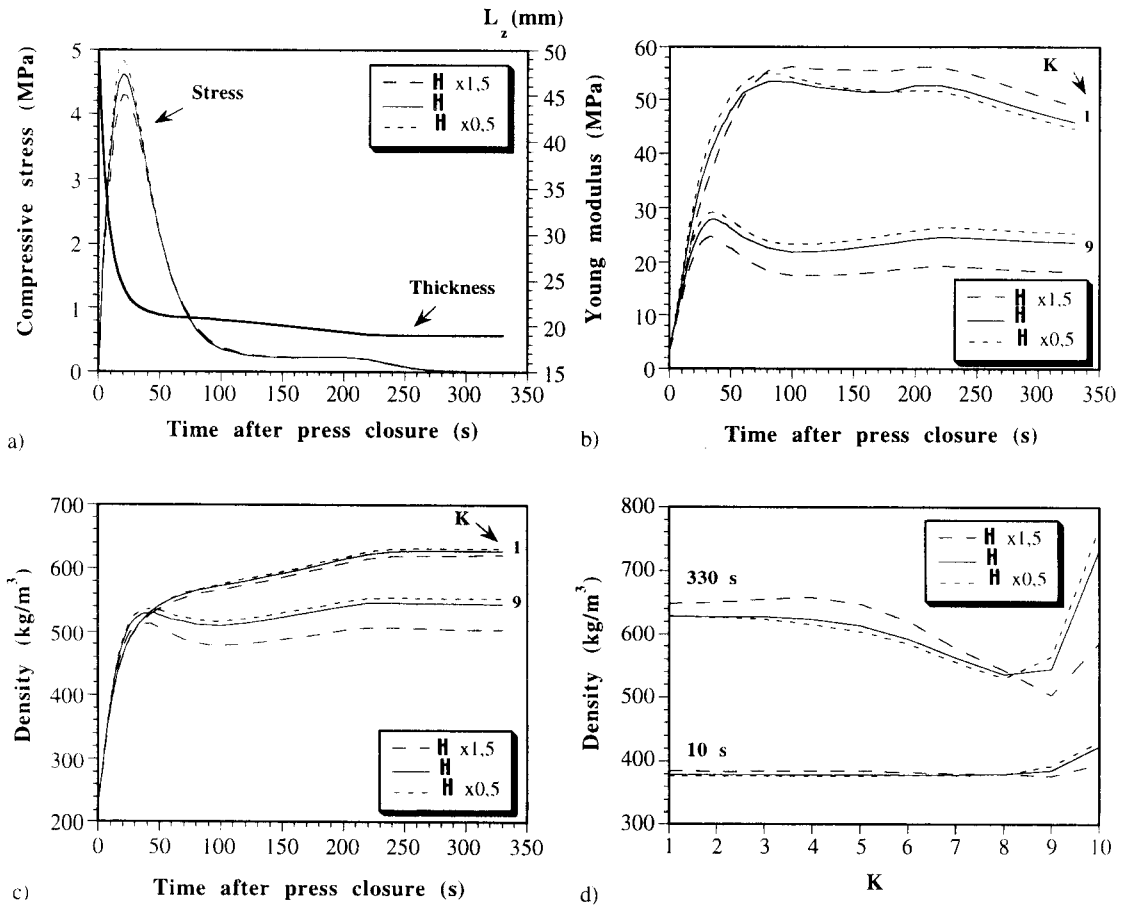


FIG. 8. Effect of initial mattress moisture content; evolution of a) overall compressive stress; b) Young's modulus; and c) density with time after press closure for several positions in the vertical direction (numbered from $K = 1$ -adjacent to board mid-plane to $K = 10$ -adjacent to board surface); d) vertical profiles of density, along the zz axis, at the board mid-plane for different times after press closure.

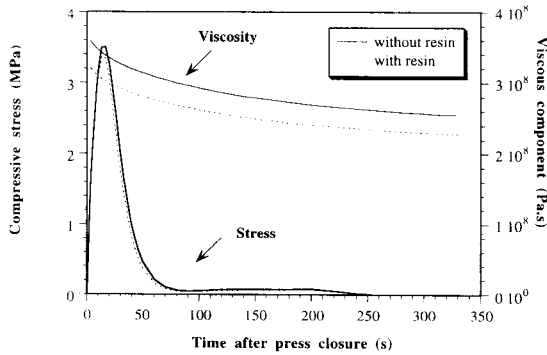


FIG. 9. Results for the viscous component of the composite estimated with and without resin: evolution of overall compressive stress with time after press closure.

MDF was carried out using SEM and mercury porosimetry. In MDF, the wood fibers are sprayed by small quantities of resin, and the forming and pressing operations orient the fibers randomly within horizontal planes parallel to the surface.

Following a three-dimensional model of heat and mass transfer previously built, two macromechanical models were developed, one assuming elastic behavior and another viscoelastic behavior. These dynamic models were used to predict the evolution of pressing pressure, strain, modulus of elasticity, and density with time at a given position in the mattress, as well as the density profiles. The elastic

model applies only at the beginning of the press cycle and it was used to show the applicability of micromechanical models to estimate local properties. We conclude that the model PPP (resin + wood fiber + gas in parallel), combined with the relationships derived for a honeycomb, is fairly effective in predicting the influence of the density of porous structure during compression. The viscoelastic model seemed to represent well the mattress consolidation during the whole press cycle, although system response is strongly influenced by the viscous component. The initial mattress moisture content has a remarkable influence on the board mechanical behavior and thus on the final density profile, whereas the effect of the platen temperature was not as important as expected. The model performance to a changing viscous component was done, assuming that the time-temperature superposition principle is valid. The choice of the Arrhenius equation for the viscous flow was found reasonable, taking into account that for the conditions of temperature and moisture content encountered in the hot-pressing of MDF, the glass transition temperature of wood polymers should not be attained. For the estimation of UF resin viscosity, no correlation was found in the literature linking this rheological property to the kinetics of cure. Nevertheless, an Arrhenius type equation was used, but this is a subject that is worthwhile exploring. For the parameters considered, the inclusion of the resin hardening leads to a slight decrease in the composite viscosity and thus to a small change on the system response, which is due to the use of an additive rule of mixtures and to the relative low resin content.

These simulation results are useful to outline the origins of stresses in the mattress and to identify the controlling factors of hot-pressing operations and to better understand the complex mechanisms involved in panel formation. The future integration of all mechanisms involved in the panel formation—the heat and mass transfer, the polymerization of the adhesive, and the rheological behavior—will permit the optimization and control of this

operation to fulfill objectives of minimization of energy consumption, better quality of the board, and increased process flexibility.

ACKNOWLEDGMENTS

This work was done under PRAXIS XXI research project number 2/2.1/TPAR/2079/95 which is gratefully acknowledged. The authors also wish to thank Dr. Vera Mata for helping with porosimetry and SEM analysis.

NOMENCLATURE

- C_2 = Linear elastic constant
- C_3 = Elastic collapse constant
- E = Young's modulus (MPa)
- E^* = Dimensionless Young's modulus
- $\langle E \rangle$ = Overall Young's modulus (MPa)
- Ho = Dimensionless elastic number
- H = Board moisture content (weight of water/weight of dry board)
- K = Spatial index in "z" direction
- L_z = Board half thickness, m
- N_z = Number of control volumes in z direction
- P = Total gas pressure, Nm^{-2}
- P_∞ = Ambient pressure, Nm^{-2}
- \mathfrak{R} = Gas constant ($8.314 \text{ kJkgmol}^{-1} \text{ K}^{-1}$)
- t = Time after press closure, s
- T = Temperature, K
- T_p = Platen temperature, K
- T_∞ = Ambient temperature, K
- T_g = Glass transition temperature, K
- Vi = Dimensionless viscoelastic number
- V = Volume fraction
- W = Mass fraction
- y_r = Resin content (weight of resin/dry-fiber weight)
- z = Spatial variable (distance along "z" coordinate)
- Z = Dimensionless spatial variable

Greek symbols

- ϵ = Compression strain
- α = Adhesive degree of cure
- Δz = Thickness of each control volume
- μ = Viscous component, Pa.s
- μ^* = Dimensionless viscous component

$\langle \mu \rangle$ = Overall viscous component, Pa·s
 ρ = Density, kg m⁻³
 ρ_c = Oven-dry board density, kg.m⁻³
 ρ_f = Oven-dry fiber density, kg m⁻³
 ρ_r = Cured resin density, kg m⁻³
 ρ_s = Solid material density, kg m⁻³
 σ = Compression stress (MPa)
 σ^* = Dimensionless ompression stress
 σ_y = Yield stress of the cellular material (MPa)
 τ = Press cycle time, s
 ζ = Relaxation time constant, s
 θ = Dimensionless time variable

Subscripts

c = composite
 f = fiber
 g = gas
 0 = reference
 r = resin
 s = solid
 i = Spatial index in x direction
 j = Spatial index in y direction
 k = Spatial index in z direction
 x = Horizontal coordinate in the length of the board (from the center of the board)
 y = Horizontal coordinate in the width of the board (from the center of the board)
 z = Vertical coordinate in the thickness of the board (from the center of the board)

REFERENCES

- AGARWAL, B. D., AND L. J. BROUTMAN. 1990. Analysis and performance of fiber composites. John Wiley & Sons, New York, NY.
- BODIG, J., AND B. A. JAYNE. 1982. Mechanics of wood and wood composites. Van Nostrand Reinhold Company, New York, NY.
- BOLTON, A., P. HUMPHREY, AND P. KAVVOURAS. 1989. The hot pressing of dry formed wood-based composites. Part VI: The importance of stresses in the pressed mattress and their relevance to the minimisation of pressing time, and the variability of board properties. *Holzforschung* 43(4):406–410.
- BUTTERFIELD, B., K. CHAPMAN, L. CHRISTIE, AND A. DICKSON. 1992. Ultrastructural characteristics of failure surfaces in medium density fiberboard. *Forest Prod. J.* 42(5):55.
- CARVALHO, L. H. 1999. Estudo da Operação de Prensagem do Aglomerado de Fibras de Média Densidade: Prensa Descontínua de Pratos Quentes. Ph.D. thesis, Universidade do Porto, Porto, Portugal.
- , AND C. COSTA. 1998. Modeling and simulation of the hot-pressing process in the production of medium density fiberboard (MDF). *Chem. Eng. Comm.* 170:1–21.
- CHARTOFF, R. P. 1997. Polymer blends and block copolymers. Pages 483–743 in A. Turi, ed. *Thermal characterization of polymeric materials*, Academic Press, San Diego, CA.
- DAI, C., AND P. R. STEINER. 1993. Compression behavior of randomly formed wood flake mats. *Wood Fiber Sci.* 25(4):349–358.
- DE BOOR, C. 1978. A practical guide to splines. Springer Verlag, New York, NY.
- DINWOODIE, J. M., C. B. PIERCE, AND B. H. PAXTON. 1984. Creep in chipboard, part 4. The influence of temperature and moisture content on the creep behaviour of a range of boards at a single stress level. *Wood Sci. Technol.* 18:205–224.
- DROZDOV, A. D. 1998. Mechanics of viscoelastic solids. John Wiley & Sons, Chichester.
- GIBSON, L., AND M. ASHBY. 1988. Cellular solids: Structure and properties. Pergamon Press, Oxford, U.K.
- HALPIN, J. C., AND S. W. TSAI. 1969. Effects of environmental factors on composite materials. AFML-TR:67–423.
- HARLESS, T., F. WAGNER, P. SHORT, D. SEALE, P. MITCHELL, AND D. LADD. 1987. A model to predict the density profile of particleboard. *Wood Fiber Sci.* 19(1):81–92.
- HATA, T., S. KAWAI, AND H. SASAKI. 1990. Computer simulation of temperature behavior in particle mat during hotpressing and steam injection pressing. *Wood Sci. Technol.* 24:65.
- HINDMARSH, A. C. 1983. ODEPACK, a systematized collection of ODE solvers in scientific computing. R.S. Stepleman et al., eds., North Holland.
- HOJJATI, M., AND S. V. HOA. 1994. Curing simulation of thick thermosetting composites. *Composites Manufacturing* 5(3):159–169.
- HUMPHREY, P., AND A. J. BOLTON. 1989. The hot pressing of dry formed wood-based composites. Part II: Simulation model for heat and moisture transfer, and typical results. *Holzforschung* 43(3):199.
- IRLE, M. A., AND A. J. BOLTON. 1991. Physical aspects of wood adhesive bond formation with formaldehyde based adhesives. *Holzforschung* 45:69–73.
- LANDAU, H. G., AND R. W. LEWIS. 1950. Heat conduction in a melting solid. *Q. Appl. Math.* 8:81–94.
- LANG, E. M., AND M. P. WOLCOTT. 1996. A model for viscoelastic consolidation of wood-strand mats. Part II. Static stress-strain behavior of the mat. *Wood Fiber Sci.* 28(3):369–379.
- LENTH, C. A., AND F. A. KAMKE. 1996a. Investigations of flakeboard mat consolidation. Part I. Characterizing the cellular structure. *Wood Fiber Sci.* 28(2):153–167.
- , AND ———. 1996b. Investigations of flakeboard

- mat consolidation. Part II. Modeling mat consolidation using theories of cellular materials. *Wood Fiber Sci.* 28(3):309–319.
- SALMEN, N. L. 1982. Temperature and water induced softening behaviour of wood fiber based materials. Ph.D. Dissertation, Dept. of Paper Tech., The Royal Inst. of Tech., Stockholm, Sweden, Paper I, p. 8
- SHALER, S. M., AND P. R. BLANKENHORN. 1990. Composite model prediction of elastic moduli for flakeboard. *Wood Fiber Sci.* 22(3):246–261.
- SUO, S., AND J. L. BOWYER. 1994. Simulation modeling of particleboard density profile. *Wood Fiber Sci.* 26:397.
- WARD, I. M., AND D. H. HADLEY. 1993. An introduction to the mechanical properties of solid polymers. John Wiley and Sons, Chichester.
- WOLCOTT, M. P., B. KASAL, F. A. KAMKE, AND D. A. DILLARD. 1989. Modeling wood as a polymeric foam: An application to wood-based composite manufacture. Pages 53–60 in Proc. Third joint ASCE-ASME Mechanics Conference, University of California, San Diego, CA.
- , F. A. KAMKE, AND D. A. DILLARD. 1990. Fundamentals of flakeboard manufacture: viscoelastic behavior of the wood component. *Wood Fiber Sci.* 22(4):345–361.
- YIN, S. 1994. Characterization par analyses thermiques de la polycondensation d'adhesifs aminoplastes et du durcissement de composites modèles bois-adhesif. Thèse Docteur, Université de Nancy I, Nancy, France.